ACS Chemical Neuroscience

Research Article

pubs.acs.org/chemneuro

Chemical Gradients within Brain Extracellular Space Measured using Low Flow Push–Pull Perfusion Sampling in Vivo

Thomas R. Slaney,[†] Omar S. Mabrouk,[†] Kirsten A. Porter-Stransky,[‡] Brandon J. Aragona,[‡] and Robert T. Kennedy*[,†]

[†]Department of Chemistry, University of Michigan, 930 N. University Ave. Ann Arbor, Michigan 48109, United States

[‡]Department of Psychology, University of Michigan, 530 Church St., Ann Arbor, Michigan 48109, United States

Supporting Information

ABSTRACT: Although populations of neurons are known to vary on the micrometer scale, little is known about whether basal concentrations of neurotransmitters also vary on this scale. We used low-flow push–pull perfusion to test if such chemical gradients exist between several small brain nuclei. A miniaturized polyimide-encased push–pull probe was developed and used to measure basal neurotransmitter spatial gradients within brain of live animals with 0.004 mm^3 resolution. We simultaneously measured dopamine (DA), norepinephrine, serotonin (5-HT), glutamate, γ-aminobutyric acid (GABA), aspartate (Asp), glycine (Gly), acetylcholine (ACh), and several neurotransmitter metabolites. Significant differences in basal concentrations between midbrain regions as little as 200 μm apart were observed. For example, dopamine in the ventral tegmental area (VTA) was 4.8 ± 1.5 nM but in the red nucleus was 0.5 ± 0.2 nM. Regions of high glutamate concentration and variability were found within the VTA of some individuals, suggesting hot spots of glutamatergic activity. Measurements were also made within the nucleus accumbens core and shell. Differences were not observed in dopamine and 5-HT in the core and shell; but their metabolites homovanillic acid (460 ± 60 nM and 130 ± 60 nM respectively) and 5-hydroxyindoleacetic acid (720 ± 200 nM and 220 ± 50 nM respectively) did differ significantly, suggesting differences in dopamine and 5-HT activity in these brain regions. Maintenance of these gradients depends upon a variety of mechanisms. Such gradients likely underlie highly localized effects of drugs and control of behavior that have been found using other techniques.

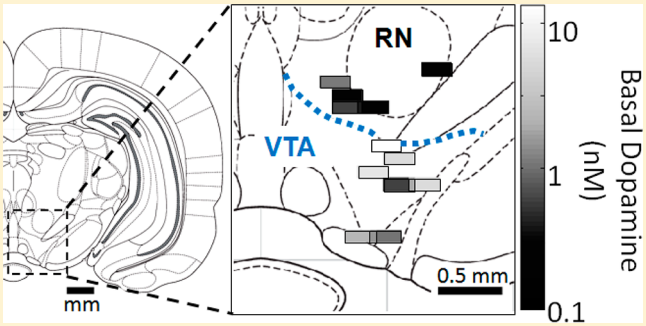

KEYWORDS: *Dopamine, glutamate, push–pull perfusion, microdialysis, spatial resolution, in vivo*

A salient feature of the brain is its heterogeneity. Neurons expressing different neurotransmitters are in close proximity and connect together in small nuclei. Neighboring nuclei and subnuclei may be involved in distinct processes providing functional significance to heterogeneous distribution. For example, a 1 mm locus of the rat nucleus accumbens (NAc) shell has been implicated in responses to hedonic stimuli.[1] Chemical analysis and histochemical imaging of brain tissue have revealed distribution of neurotransmitters,[2,3] processing enzymes,[4,5] receptors,[6,7] and reuptake proteins[2,8,9] that presumably underlie functional heterogeneity in the brain. Although these approaches give an important view of brain organization, they do not provide distribution of neurotransmitters where they are actually active, that is, in the extracellular space. It would be difficult to predict differences in extracellular concentration because of complex regulation of neurotransmitters by combined effects of synthesis, release, reuptake, and metabolism.[10−12] Direct, spatially resolved measurement of neurotransmitter extracellular concentration is required to address this issue. Such measurements also provide a means to assess the regulation of a neurotransmitter, its transport through the brain, and its potential for extrasynaptic signaling (i.e., "volume transmission").[13] In this work, we demonstrate a method to measure extracellular concentrations of neurotransmitter and metabolites with 0.004 mm^3 (4 nL) resolution to reveal gradients across the boundary between several nuclei.

Common methods for in vivo measurement include microdialysis[14] and microelectrodes.[15] Because microdialysis probes are 200−400 μm diameter with a 1−4 mm long sampling membrane, they provide a relatively gross measure of chemical distributions. Microelectrodes can be made much smaller; however, direct measurement of basal concentration is often confounded by background interference. Nevertheless, differences in dopamine (DA) activity have been detected across ∼150 μm distances by electrochemical methods.[16−18]

In this work, we apply low-flow push–pull perfusion sampling[19] to make spatially resolved measurements in brain extracellular space. This method is similar to classic push–pull

Received: September 13, 2012
Accepted: November 12, 2012
Published: November 12, 2012

perfusion wherein sampling is achieved by infusing physiological buffer and withdrawing sample at equal flow rates through closely spaced capillaries.[20] By using low flow rates (50 nL/min) and smaller capillaries, spatial resolution is enhanced relative to conventional push−pull perfusion.[19,21−23] Fractions collected from probes in this work are analyzed using a recently developed liquid chromatography−mass spectrometry (LC-MS) method to assay 13 neurotransmitters and metabolites.[24]

The method is used to measure extracellular chemical gradients across a few hundred micrometers in three brain regions where DA distributions are expected. We focus on DA because of interest in this neurotransmitter for its role in reward, addiction, and certain diseases.[25,26] Also, substantial effort has already been expended in evaluating its extracellular concentration and heterogeneity[17,27−29] allowing comparison to previous studies.

One set of measurements is made across the corpus callosum at the boundary between cortex and striatum. DA neurons are present in both cortex and striatum, but much richer DA innervation in the striatum than cortex suggests the potential for a sharp concentration gradient.[2] Measurements are also made at the border of ventral tegmental area (VTA) and red nucleus (RN) where a similar gradient is expected based on strong DA innervation of VTA relative to RN.[26] Finally, we also made spatially resolved measurements within the NAc. Functional and morphological heterogeneity within the NAc has implications for addiction and disease pathologies.[2,30,31] The dorsolateral accumbens, or core, projects to brain regions associated with motor activity, while the ventromedial accumbens, or shell, projects to regions associated with the limbic system.[2] Dopaminergic neurons are found throughout the NAc; however, dopaminergic projections to the core originate within parabrachial VTA and substantia nigra pars compacta, whereas projections to the medial shell originate within paranigral VTA.[27,32] A consensus on differences in basal concentration of DA within the NAc has not been reached with studies finding higher, equal, or lower concentrations in core versus shell.[27] The variability in microdialysis observations has been attributed to probe placements and angles of implantation,[27] emphasizing the significance of spatial resolution.

Although this study centers on detection of likely gradients in DA, the measurement of other neurotransmitters and metabolites provides further insight into chemical heterogeneity within these regions. Further, the measurements provide a validation of the push−pull method for spatially resolved chemical measurements.

RESULTS AND DISCUSSION

Polyimide-Encased Push−Pull Probe. A novel push−pull probe design, compatible with commercially available microdialysis cannulae, was used for this work (Figure 1). Previous side-by-side push−pull probes housed sampling and infusion capillaries within a hypodermic needle;[21,23] however, the needle sheath perturbed tissue ventral to the probe inlets and increased probe diameter to approximately twice that of the probe capillaries (400 μm versus 180 μm[21]). To avoid these problems, we made probes that consisted of two fused silica capillaries sheathed in polyimide tubing. Polyimide was used because it is biocompatible[33] and available as thin wall (20 μm) tubing. The tip of the probe was polished to provide a smooth surface and unobstructed path between push outlet and pull inlet (Figure 1c and Methods). The resulting probes are easily made, smaller than previous designs,[21] and in principle avoid tissue damage from a protrusion below the sampling zone.

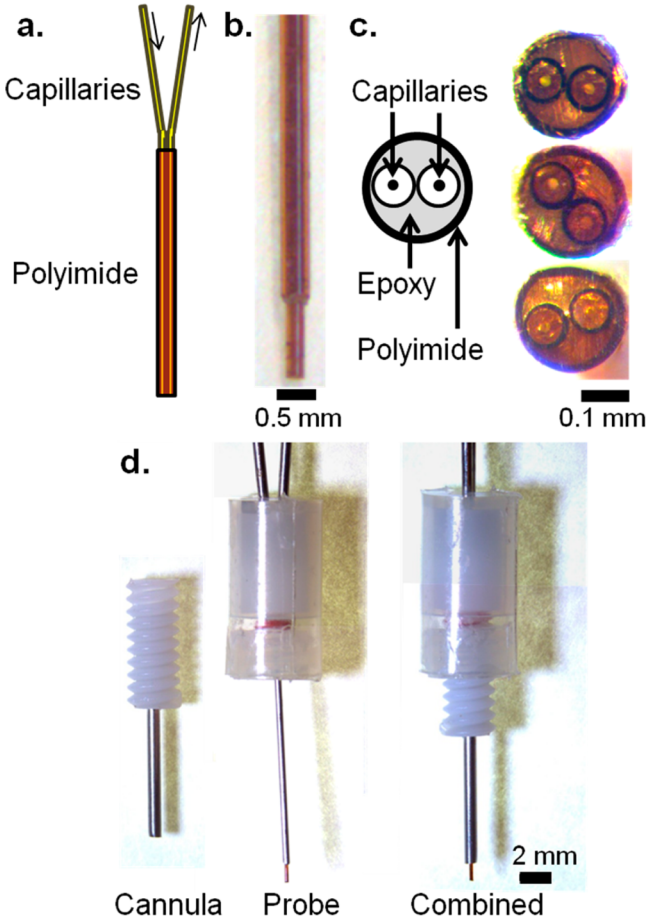

Figure 1. Low flow push−pull perfusion probes. (a) Schematic of a polyimide-encased side-by-side capillary probe. The space within the polyimide is filled with epoxy. (b) Side view of a probe used in anesthetized studies, with a 360 μm OD capillary to add rigidity. (c) Polished tips of three probes, showing the polished capillaries, epoxy, and polyimide. (d) Probe assembly for awake, freely moving studies. When inserted, the probe protrudes 1 mm past the tip of the cannula into the brain.

To estimate spatial resolution of sampling (i.e, the volume of tissue sampled by a probe), a probe was inserted into agar gel impregnated with the fluorescent dye resorufin. Fluorescence imaging of the probe tip during push−pull operation allowed visualization of the sampling field as a localized region of resorufin depletion (Figure 2). A plot of fluorescence signal along a line perpendicular to the probe tip (Figure 2c) shows that depletion of resorufin extends about 200 μm beyond the tip, but at 100 μm resorufin is about 80% of the bulk concentration. We estimate that the sampled volume is 0.004 mm^3 (4 nL) by assuming a cylindrical sampling field, with diameter of 220 μm and height of ∼100 μm, centered over the push−pull lumen. Because dilute agar prevents convection, this volume represents spatial resolution for an analyte affected only by diffusion, similar to brain tissue.[34−36] The spatial resolution in vivo may be even higher because active processes, such as reuptake and metabolism, may reduce the distance that a molecule could diffuse in the brain space. Thus, a molecule released within the diffusion controlled sampling field may never reach the probe because of these processes.[37]

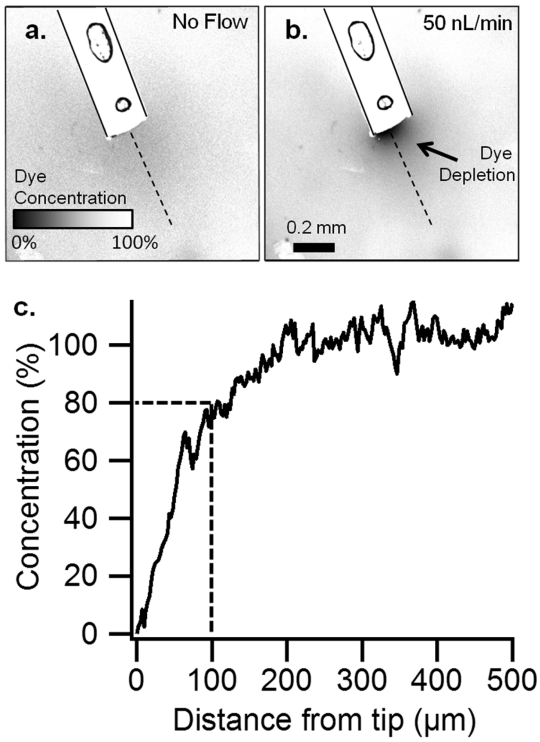

Figure 2. Determination of spatial resolution by low flow push−pull perfusion in vitro. Confocal microscopy of a probe (outlined) in agar containing 1 μM resorufin (a) without sampling and (b) push−pull sampling at 50 nL/min. (Circles are air bubbles within the probe epoxy.) (c) The relative concentration of resorufin in a linear path (dashes in A,B) from the tip of the probe, measured by the difference in fluorescence. Scale bar is 200 μm.

Probe Recovery. In vitro recovery at 37 °C was 93 ± 17% for Glu and 89 ± 14% for DA (n = 3) from a stirred vial and 69 ± 4% for Glu and 51 ± 15% for DA (n = 3) from an unstirred vial. Microdialysis experiments have shown that recovery measurements from a stirred vial more closely emulates the in vivo condition.[38] The high recovery is comparable to previously observed values for push−pull perfusion[19,21,22] and is a benefit of not having a membrane to limit mass transport (as with microdialysis) and use of low flow rates.[34] Concentrations reported in this paper are not corrected for relative recovery.

Measurement of Concentration Gradients within Anesthetized Animals. To evaluate a region likely to have DA gradients, samples were collected at 500 μm steps near the border of cortex, corpus callosum, and striatum in 3 animals (Figure 3a−c, Table 1). DA concentration changed over short distances and was higher within the dorsal striatum (1.7 ± 0.2 nM) than corpus callosum (0.4 ± 0.2 nM) and cortex (0.4 ± 0.2 nM). The extracellular concentration gradient matches the distribution of DA neurons, which have a much greater population within the striatum than cortex or corpus callosum.[2]

As shown in Figure 3d and Table 1, no other compounds showed significant differences except the DA metabolite 3-MT which varied from 0.35 ± 0.03 nM to 0.10 ± 0.01 nM to 0.08 ± 0.02 nM for striatum, corpus callosum, and cortex, respectively (p < 0.001, one-way ANOVA with Tukey's multiple comparisons test). Although DOPAC and HVA were equivalent at different locations, we did find that the ratio of HVA to DOPAC concentration correlated with probe depth

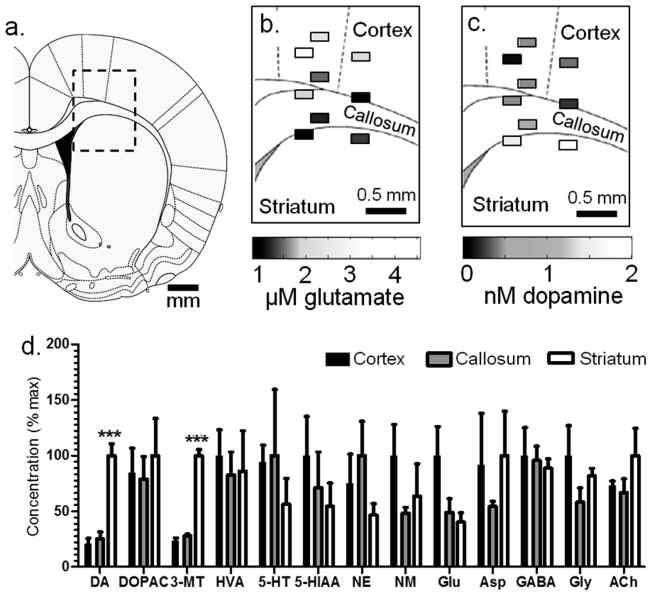

Figure 3. Comparison of measurements taken from multiple locations within anesthetized animals. (a) Sampling was conducted at the cortex, corpus callosum, and striatum boundary.[63] The rectangle diameters represent the probe width (220 μm) and a conservative estimate of tissue sampled (100 μm). Probe placements were mapped, and concentration measurements at each site are shown for (b) Glu and (c) DA. Vertically aligned fractions represent one animal. (d) Differences in neurotransmitters were observed, expressed as the normalized mean ± SEM (***p < 0.001, one-way ANOVA, Tukey's multiple comparisons test).

Table 1. Basal Extracellular Concentrations (nM): Anesthetized Rats

	cortex	corpus callosum	striatum[a]
DA	0.4 ± 0.1	0.4 ± 0.1	1.7 ± 0.2***
DOPAC	47 ± 12	44 ± 11	55 ± 18
3-MT	0.08 ± 0.01	0.10 ± 0.00	0.35 ± 0.02***
HVA	36 ± 8	29 ± 7	31 ± 13
5-HT	0.4 ± 0.1	0.4 ± 0.2	0.2 ± 0.1
5-HIAA	43 ± 15	31 ± 14	24 ± 9
NE	0.8 ± 0.3	1.1 ± 0.3	0.5 ± 0.1
NM	0.2 ± 0.1	0.1 ± 0.0	0.1 ± 0.1
Glu	2600 ± 700	1300 ± 300	1100 ± 200
Asp	590 ± 300	350 ± 30	640 ± 260
GABA	44 ± 11	43 ± 6	39 ± 4
Gly	5400 ± 1500	3200 ± 700	4400 ± 400
Ach	31 ± 2	28 ± 5	42 ± 10

[a]***p < 0.001, one-way ANOVA with Tukey's multiple comparisons test versus both the corpus callosum and cortex.

(Figure 4a). These results are in agreement with previous microdialysis observations from awake rats which found HVA/DOPAC of 1.2 within the cortex and 0.7 within the striatum.[39]

Regional differences in DA metabolite concentrations offer insight into not only DA abundance but its turnover and extracellular fate. Among DA metabolites, 3-MT is most correlated with DA release because it is formed only extraneuronally by catechol-O-methyltransferase (COMT).[40] DOPAC is formed primarily within the presynaptic neuron and is therefore a measure of intraneuronal turnover.[41] The chemical profile suggests higher DA release and tone in the striatum (higher 3-MT and DA concentration), but greater

dx.doi.org/10.1021/cn300158p | ACS Chem. Neurosci. 2013, 4, 321−329

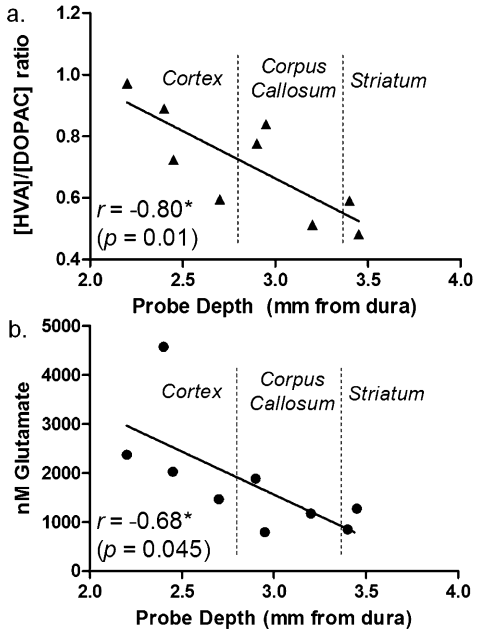

Figure 4. Spatial distrubtion of neurochemicals along a single track from cortex to striatum in anesthetized rats. (a) HVA/DOPAC ratio (indicative of extraneuronal or intraneuronal DA metabolism) varied across the cortex, corpus callosum, and striatum. (b) A gradient of decreasing Glu was also observed as a function of probe depth at this boundary (n = 3 rats, three measurements per rat).

intraneuronal turnover within the cortex (as DOPAC concentrations are comparable despite much lower DA in cortex). HVA formation requires extraneuronal metabolism by COMT, so the ratio of HVA to DOPAC can offer insight to whether extraneuronal metabolism or reuptake is dominant for removal of DA from extracellular space.[41,42] Because DA reuptake is generally faster than metabolism, the HVA/DOPAC ratio has also been considered an indirect indicator of extracellular DA lifetime.[42] If correct, then the higher HVA/DOPAC ratio in cortex suggest greater DA lifetime there, in agreement with lower DAT expression in that brain region.[8] It is interesting that a gradient of 3-MT is maintained over such a short distance. The maintenance of this gradient may be aided by high monoamine oxidase (MAO) abundance in the corpus callosum[4,43] which could degrade 3-MT.

Among other compounds, Glu showed some differential distribution. Glu concentration in the cortex was 2.4-fold greater than that in the striatum (2.6 ± 0.7 μM versus 1.1 ± 0.2 μM). Although this difference did not reach statistical significance, Glu concentration did have a significant correlation with probe depth (Figure 4b, $p < 0.05$, Pearson's $r = 0.678$), suggesting a decreasing concentration gradient passing from cortex to striatum. This observation agrees with previous microdialysis studies which found basal concentrations of Glu to be ~2-fold higher within the cortex than striatum; however, the sizes of the probes used in that work (2−5 mm active length) precluded observations of the gradual gradient across the callosum seen here.[44,45] Interestingly, the higher concentration of Glu correlates with greater abundance of glial Glu transporters (GLAST and GLT-1) in the cortex relative to the striatum.[46] Because GLAST and GLT-1 remove Glu from extracellular space, these results suggests higher Glu release in cortex to achieve the higher Glu tone.

Gradients in Neurochemicals in the Dorsal VTA. Gradients of extracellular neurochemicals were examined in the VTA and dorsal of the VTA (RN) of awake, freely moving rats (Figure 5). Because these experiments were performed in awake animals, only one probe placement was made per animal. (Micropositioners are available that may allow multiple placements in awake subjects; but for these experiments we used a single position per animal to avoid the complication of moving a probe in an awake subject.) Experiments grouped as VTA were primarily collected from the parabrachial pigmented nucleus (n = 6) but included one experiment from the parainterfascicular nucleus and one from the rostral part of the ventral tegmental area. Experiments grouped as RN were collected from the red nucleus parvicellular part (n = 3) and the prerubral field (n = 2). No significant differences were observed between subnuclei.

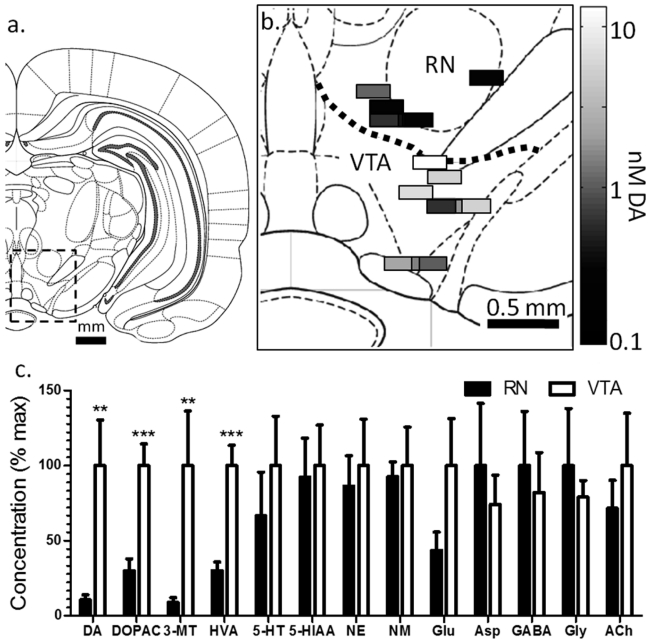

Figure 5. Spatial distribution of neurochemicals around VTA and RN in awake rats. (a) Coronal map of the brain showing the location of the VTA and RN and (b) placements of measurements made in the VTA and RN with the DA concentration at each. Samples represent A/P coordinates of 4.80 mm to 5.64 mm posterior to bregma, plotted at 5.28 mm and excluding 1 fraction from the rostral area of the VTA for clarity. (c) Normalized concentrations ± SEM between the VTA and RN.

Basal concentrations of DA were much higher within the VTA (4.8 ± 1.5 nM, n = 8) than within the RN (0.5 ± 0.2 nM, n = 5) reflecting rich dopaminergic innervation of the mesolimbic system within the VTA relative to RN.[26] As shown in Figure 5b, this concentration difference is visible between even the most dorsal region of the VTA and the most ventral of the RN (200 μm apart). The sharp concentration gradient, similar to that seen for cortex-striatum, supports the notion of strong regulation of the diffusion of DA through extracellular space. In contrast to what was observed with the cortex-striatum boundary, all DA metabolites are also significantly more abundant within the VTA than RN (see Table 2): DOPAC was 3-fold higher ($p < 0.001$), 3-MT was 11-fold higher ($p < 0.01$), and HVA was 3-fold higher ($p < 0.001$). These results suggest mechanisms that prevent DA metabolites

dx.doi.org/10.1021/cn300158p | ACS Chem. Neurosci. 2013, 4, 321−329

Table 2. Basal Extracellular Concentrations (nM): Awake, Freely Moving Rats

	VTA	RN[a]	core	shell[a]
DA	4.8 ± 1.5	0.5 ± 0.2**	7.2 ± 1.2	11 ± 4
DOPAC	220 ± 30	65 ± 17***	1100 ± 330	720 ± 110
3-MT	3.5 ± 1.3	0.30 ± 0.11**	0.80 ± 0.29	0.66 ± 0.12
HVA	150 ± 20	44 ± 8***	460 ± 60	130 ± 30***
5-HT	1.6 ± 0.5	1.1 ± 0.5	1.3 ± 0.6	0.6 ± 0.2
5-HIAA	430 ± 120	400 ± 110	720 ± 200	220 ± 50*
NE	2.5 ± 0.8	2.2 ± 0.5	2.5 ± 1.1	1.0 ± 0.3
NM	0.7 ± 0.2	0.6 ± 0.1	0.4 ± 0.1	0.4 ± 0.1
Glu	8500 ± 2700	3700 ± 1000	2400 ± 900	930 ± 340
Asp	1500 ± 400	2000 ± 800	1100 ± 500	450 ± 190
GABA	160 ± 50	190 ± 70	150 ± 110	92 ± 48
Gly	7200 ± 1000	9200 ± 3500	4400 ± 1100	2100 ± 500
ACh	9.5 ± 3.3	6.8 ± 1.8	10 ± 3	7.3 ± 2.1

[a]*$p < 0.05$; **$p < 0.01$; ***$p < 0.001$ for comparison of VTA to RN or NAc core and shell; Student's t test of adjacent nuclei.

from diffusing to adjacent nuclei. Such mechanisms may include clearance from extracellular space by neurons, glia, or vasculature. The ratio of HVA to DOPAC was not significantly different between the VTA and RN (0.66 ± 0.05 versus 0.75 ± 0.09 respectively), despite differences in DAT distribution.[47]

Among other compounds measured, only Glu showed potential spatial heterogeneity of concentration (Figure 5c). The basal concentration of Glu was ∼2-fold greater within the VTA than the RN; however, this difference did not reach statistical significance because of high variability in the VTA. Glu concentration ranged from 2 and 24 μM (median 5.6 μM) within VTA (n = 8) compared to the 2−7 μM (median 3.4 μM) within the RN (n = 5). The variance was significantly greater in VTA than RN ($p < 0.05$, F-test). We also found that sequential fractions collected within the VTA of a given animal had higher variability than the RN, with a relative standard deviation of 65 ± 23 in the VTA as compared to 37 ± 14 in the RN ($p < 0.05$, t test). The high concentration and variability suggest a high degree of glutamatergic activity with these specific placements. It is unclear if the elevated activity is an individual difference or "hot spots" within the VTA. These data may indicate localized regions of elevated glutamatergic neuronal activity. They may also relate to distribution of non-neuronal sources of Glu such as the cystine-glutamate antiporter, which has been found to cluster in some brain regions.[10,48] Another possible reason for the variable Glu in the VTA is tissue damage caused by the probe, for example, disruption of neurons could cause release of intracellular Glu. This explanation is discounted because we have previously observed that Glu concentration in perfusate is elevated immediately after push−pull probe insertion into brain tissue and that it decreases and to a stable level within 0.5 h.[22,23] Similar findings on microdialysis have been reported[49] and is attributed to the disruption of neurons and subsequent dissipation of the neurotransmitters. Thus, sampling in these experiments has occurred after Glu released by cell disruption has been removed. Further, the variation of Glu was far stronger in the VTA than other brain regions and it seems unlikely that damage associated with the probe would have such disparate effects on different brain regions.

Spatial Differences in the Nucleus Accumbens. Differences in DA concentration between the NAc core and shell is still unsettled because of difficulty of making spatially resolved measurements.[27] To address this issue, we sampled from 11 animals with probe placements in core (n = 5) and shell (n = 6) as shown in Figure 6. The small size of the probes means that sampling was completely within a specified brain region, thus eliminating uncertainty associated with larger probes that may sample from a larger area. Using this method, we found no significant difference between core and shell DA, DOPAC, or 3-MT (Figure 6, Table 2); however, HVA concentration was 3-fold higher within the core than shell ($p < 0.001$). As a result, the ratio of HVA to DOPAC was higher ($p < 0.01$) within the core (0.53 ± 0.09) than shell (0.19 ± 0.02). The greater HVA within the core suggests greater turnover of DA in the core than shell. The differences in HVA/DOPAC ratio indicate greater intraneuronal than extraneuronal metabolism within the shell and are suggestive of greater DA lifetime in the core.[42] This result is surprising given the higher abundance of DAT within the core than shell, but has been observed previously by measuring clearance rates of exogenous

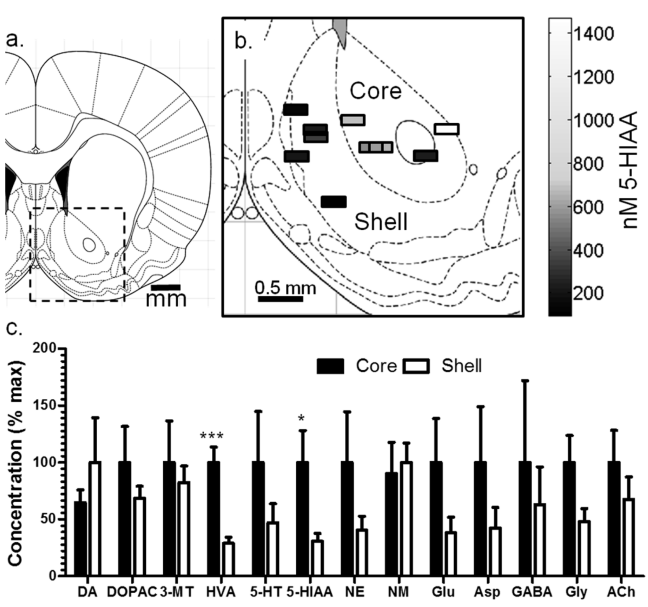

Figure 6. Spatial distribution of neurochemicals around within the NAc core and shell in awake rats. (a) Coronal map of the brain showing the nucleus accumbens and (b) placements of 5-HIAA measurements made in the core and shell with the concentration at each. Probes varied from 1.32 to 2.52 mm anterior to bregma but are shown at 1.80 mm anterior to bregma for clarity. (c) Normalized concentrations ± SEM between the accumbens core and shell.

dx.doi.org/10.1021/cn300158p | ACS Chem. Neurosci. 2013, 4, 321−329

DA and may relate to regional differences in DAT activity.[50] The shorter extracellular lifetime of DA within the shell may correlate with the much greater behavioral responses observed with local application of DA reuptake inhibitors to the shell than core.[29] Indeed, while these regions are just a few hundred micrometers apart, voltammetry studies show that their neurochemical activation to cues and drugs varies substantially.[30,31] We cannot rule out DA hot spots within either nucleus without more extensive mapping as has been suggested by voltammetry studies.[51]

The results also suggest greater 5-HT activity in core than shell. 5-HT was 2.2-fold higher in the core; however, the concentration difference did not reach statistical significance. Supporting the idea of differences in 5-HT activity though, 5-HIAA was 3-fold higher in the core ($p < 0.05$). Previous studies have been inconclusive on whether 5-HT activity is different between these two regions. Microdialysis sampling did not find a significant difference in 5-HT concentration between NAc core and shell[29,52] even though the shell contains a greater number of 5-HT neurons and the core contains more of the 5-HT transporter SERT.[2,3] In view of the higher 5-HIAA and SERT abundance in the core, it is reasonable to postulate that more 5-HT is released in the core than shell, but greater reuptake and metabolism keep the extracellular concentration similar in the two brain regions. As 5-HT neurons of the core are more vulnerable to drugs of abuse than those of the shell,[2] selectively studying 5-HT within the core may provide new insights in addiction.

A significant difference in NE and its metabolite NM between core and shell was not observed, whereas previous microdialysis work observed higher NE concentrations in the shell.[27] This difference may relate to probe placement. Dopamine-β-hydroxylase (DBH) distribution, indicative of NE synthesis, indicates only partial innervation of the shell, favoring the caudal portion with NE neurons.[5] Examination of results from individual probe placements supports this notion. The lowest concentration of NE (0.1 nM) was observed within the most rostral spot sampled (2.52 mm anterior to bregma), and two of the three highest concentrations in the most caudal spots sampled (1.4 and 1.2 nM at 1.32 mm anterior to bregma). A more direct study of these differences is required to establish if this trend is statistically significant.

Comparison to Microdialysis Concentrations. The high recovery by low flow push−pull perfusion in vitro suggests that the recovered concentrations may approximate actual extracellular concentrations. Presently, the most accepted method for measuring basal concentrations is by calibrated microdialysis measurements.[53,54] Recovered concentrations of amine neurotransmitters were similar to those reported previously by microdialysis calibrated by "no-net-flux" (NNF) (see Table 1 in Supporting Information for summary of values used for comparison). NNF values for DA were 5.0 nM in the VTA,[55] 4.7−8.3 nM in NAc (across both core and shell),[56−58] and 2.5−6.5 nM in the striatum of anesthetized rats,[59,60] all close to the push−pull values (see Tables 1 and 2, and Table 1 in the Supporting Information). NNF measurements of 5-HT within the accumbens were 0.6−0.7 nM,[57,58,61] whereas push−pull measurements averaged 0.9 ± 0.3 nM. In contrast to the good agreement found for amines, amino acids showed more differences. GABA in NAc was ∼33 nM by NNF but 3−5 times that (depending on subregion) by push−pull. Glu concentrations agreed well for NAc core but differed by 5-fold for NAc shell, 3-fold in striatum, and ∼2-fold in VTA. Glu concentrations were both higher and lower by NNF, depending on brain region, than by push−pull sampling. Without further study, it is difficult to tell if these differences are due to lack of calibration for current method, spatial resolution, differences in probe impact, or other factors.

Probe Placement and Tissue Damage. For all in vivo experiments, probe placement was confirmed by injecting dye through the probe and examining coronal brain slices (see Methods for details and Supporting Information Figure 1 for example). While this approach has limits, it does allow confirmation that the probe was positioned within the brain regions and subregions reported. The histological images also allow a preliminary evaluation of tissue damage caused by the probes. Substantial tissue disruption is apparent along the cannula track and dorsal of the probe tip; however, around the probe tip, no obvious cellular destruction or brain morphology disturbance is apparent. This result is agreement with a previous report[19] and in contrast to observations made with higher flow push−pull perfusion.[62] In view of the potential utility of this sampling method, a detailed study of its effect on tissue is warranted.

■ CONCLUSIONS

Low-flow push−pull perfusion allows high spatial resolution chemical measurements to be made in the brain. When combined with LC-MS the method allows a relatively comprehensive study of chemical gradients in the brain. The results show that gradients in basal concentration of neurotransmitters and metabolites can exist between adjacent brain regions less than 1 mm apart. Gradients appear to be controlled by different mechanisms depending on the brain region. Cortical and striatal DA neurons operate differently with higher release and shorter lifetime in the striatum. A mechanism that prevents transport of DA metabolites from the VTA to adjacent brain regions is active. Among the most intriguing findings are high variability of Glu within the VTA which may indicate hot spots and/or individual differences. High temporal resolution measurements will be useful to further characterize such hot spots and determine their functional significance. Within the NAc, differences in DA and 5-HT activity are apparent, based on the differences in metabolite concentrations despite similar neurotransmitter concentration, between the core and shell which may explain differences in susceptibility to some drugs. The ability to measure such gradients will help determine their role in highly localized effects of drugs and behavioral control that has been found with other techniques.

■ METHODS

Materials and Reagents. Unless otherwise specified, all reagents were purchased from Sigma Aldrich (St. Louis, MO). Fused silica capillaries were purchased from Polymicro (Phoenix, AZ). Unions for 360 μm outer diameter (OD) capillaries were purchased from Idex Health and Science (P-772, Oak Harbor, WA). Polyimide tubing was purchased from Smallparts.com (Seattle, WA). Thixotropic epoxy was purchased from Epoxy Technology (353ND-T, Billerica, MA). Cyanoacrylate glue was purchased from K & R International (E-Z Bond, Laguna Niguel, CA). Artificial cerebrospinal fluid (aCSF) contained 145 mM NaCl, 2.68 mM KCl, 1.01 mM $MgSO_4$, 1.22 mM $CaCl_2$, 1.55 mM Na_2HPO_4, and 0.45 mM NaH_2PO_4, pH 7.4.[22]

Probe Fabrication. For anesthetized experiments, probes were fabricated from two 20 μm inner diameter (ID), 90 μm OD capillaries. These capillaries were coated with thixotropic epoxy and inserted through a 3 cm length of 180 μm ID, 220 μm OD polyimide tubing. Excess epoxy was gently wiped off and the epoxy cured for 1 h at 50

°C and 20 min at 80 °C. The polyimide and capillaries were cut within 3 mm of the end of the polyimide. Adapters consisting of 2 cm lengths of capillary (150 μm ID, 360 μm OD) were glued with cyanoacrylate on both probe capillaries for a probe length of 10 cm. Excess 90 μm OD capillary was cleaved flush with the 360 μm OD adapter using a ceramic capillary cutter.

To polish the probe, each capillary was flushed with 0.5 μL/min of water and the tip was pressed against wet 1500 grain sand paper fixed to a 1 Hz rotating polishing wheel (BV-10, Sutter Instrument Co., Novato, CA). A 2 cm length of 250 μm ID, 360 μm OD capillary was glued over the polyimide to increase rigidity leaving 1 mm exposed at the probe tip.

Probes for awake, freely moving animal experiments were fabricated the same as the anesthetized probes except that they consisted of two 60 cm lengths of 40 μm ID, 100 μm OD capillaries and 200 μm ID, 240 μm OD polyimide tubing. These tubes were threaded through 45 cm of 0.50 mm ID, 1.52 mm OD Tygon tubing (Saint-Gobain, Courbevoie, France), and the tip was inserted through a threaded probe holder (C312ICP/O/SPC, Plastics One, Roanoke, VA). A 1.2 cm 26 gauge hypodermic tubing (BD, Franklin Lakes, NJ) was placed over the probe and glued 1 mm from the tip with cyanoacrylate. The probe was fixed to the holder by gluing to a ∼6 mm length of Tygon placed partially over the metal inlet tube of the probe holder, and the length was chosen to allow 1 mm to protrude from the cannula when inserted. The 26 gauge tubing did not protrude from the cannula when inserted, as shown in Figure 1d.

Surgical Procedures. All surgical procedures were performed according to a protocol approved by the University Committee for the Use and Care of Animals. Male Sprague−Dawley rats weighing between 250 and 300 g were anesthetized using 65 mg/kg ketamine and 0.25 mg/kg dexdomitor i.p. For awake experiments, a stainless steel cannula was inserted to 1 mm dorsal to the region of interest (C312GP/O/SPC, 8 mm, Plastics One, Roanoke, VA). For the VTA and RN experiments, cannulae were implanted at 5.3 mm posterior and 1.0 mm lateral to bregma and to 5.8 or 6.8 mm from dura for the RN or VTA, respectively. For the accumbens, cannulae were implanted at 1.2 or 1.8 mm anterior and 1.4 or 0.8 mm lateral to bregma for the NAc core or shell, respectively. Cannulae were implanted to a depth of 5.8 mm from dura. Three screws were inserted in the skull near the cannula and a cap was fabricated from methyl methacrylate (Teets Cold Cure Denture Material, Co-oral-ite Dental Mfg. CO, Diamond Springs, CA). A small metal clip was also inserted into the cap for attaching the tether. A stylet (C312DC, Plastics One, Roanoke, VA) was inserted into the cannula and the animal was allowed at least 48 h to recover.

For anesthetized experiments, animals were administered ketamine and dexdormitor (as above) with boosters (22 mg/kg ketamine, 0.08 mg/kg dexdomitor) as needed and the probe was fixed to the stereotaxic arm. The animal was placed in an ultraprecise stereotaxic frame (David Kopf, Tujunga, CA). A burr hole was drilled above the region of interest, and the probe was slowly lowered (approximately 10 s per mm) while backflushing both capillaries with aCSF at 500 nL/min. When the desired depth was reached, the backflushing was decreased gradually over 30 s to 50 nL per minute per capillary, and was backflushed for 8 min prior to starting the "pull" flow. Depths of 2.0, 2.5, and 3.0 mm from bregma were targeted for each animal, and backflushing was used while lowering between depths.

Probe placements were identified by infusing dye through the sampling probe and performing histological analysis of the tissue. After a sampling experiment was complete, 100 nL of either Evans Blue (0.24 mg/mL in aCSF) or a filtered, saturated solution of FastGreen FCF in aCSF were infused at 50 nL/min. FastGreen was preferred because it preferentially labeled the probe track whereas Evans Blue uniformly labeled the entire tissue volume affected by the dye around the probe tip. Brains were fixed in 10% paraformaldehyde containing 2.5% sucrose and 100 mM phosphate buffered saline for at least 24 h. Brains were then frozen and sliced along the coronal plane to find the probe track. Slicing with a cryostat and manual slicing with a razor were both utilized. Manual slicing provided facile visualization of anatomical features for mapping placements and rapid preparation time. Cryostat slices (60 μm thick) were preferred as they were of better uniformity and reproducibility than manual slices and could be stored on slides for later review (Superfrost Plus, Fisher Scientific, Fairlawn, NJ). Probe placement was considered to be the point at maximal dye concentration for Evans Blue, or the base of the probe track for FastGreen. Brain regions were identified by reference to the atlas of Paxinos and Watson.[63] Anatomical boundaries and white matter (such as the anterior commissure in the nucleus accumbens, or the mesolateral lemniscus in the VTA) were used as landmarks to aid identification of probe location. Supporting Information Figure 1 illustrates two examples of histological analysis used to identify probe placement.

Freely Moving Experiments. Following cannulation and recovery, rats were placed in a Raturn (Bioanalytical Systems, West Lafayette, IN) and allowed free access to food and water. To implant the probe, rats were briefly anesthetized with isoflurane vapor and the stylet removed. While backflushing at 500 nL/min through each capillary, probes were gently inserted into the cannula and slowly tightened at ∼1 turn per 5 s, making sure to prevent any twisting. Immediately after implanting, the probe backflushing was reduced to 50 nL/min for 8 min.

Sample Collection and Analysis. To start "pull" flow, a 13 cm length of 100 μm ID, 360 μm OD capillary was connected to one of the probe capillaries, and sufficient vacuum to fill this tube at 9.4 s/mm (equal to 50 nL/min) was applied. Samples collection was initiated after 1 h of perfusion to allow for tissue recovery.[21] Sampling was conducted for approximately 3 h (∼9 fractions) for awake animals, or 1 h (3 fractions) at each depth for anesthetized. Fractions were transferred from 1 μL collection capillaries to low-volume autosampler vials and were immediately derivatized as described previously.[24] The following reagents were added with intermediate vortexing in rapid succession: 1.5 μL of 100 mM sodium tetraborate, 1.5 μL of benzoyl chloride (2% in acetonitrile), 1.5 μL of $_{13}$C-internal standard, and 1 μL of 100 nM d4-ACh in water.

The ^{13}C-internal standard reagent contained 1% (vol) of a ^{13}C-benzoyl chloride derivatized stock solution (described in detail elsewhere[24]), 97% dimethyl sulfoxide, and 2% acetic acid. Calibration curves were prepared for each analyte in aCSF with the following concentrations: 0.5, 5, 10, 50, and 100 nM for DA, NM, NE, 5-HT, and ACh; 5, 10, 50, 100, and 1000 nM for DOPAC, HVA, 5-HIAA, Glu, GABA, and Asp; and 50, 100, 500, 1000, and 10 000 nM for Gly.

■ ASSOCIATED CONTENT

Supporting Information

Illustration of histology for mapping probe placements following sampling and dye infusion. Table for comparison of basal perfusate concentrations and no-net-flux microdialysis concentrations. This material is available free of charge via the Internet at http://pubs.acs.org/.

■ AUTHOR INFORMATION

Corresponding Author

*Telephone: 1-734-615-4363. E-mail: rtkenn@umich.edu.

Author Contributions

T.R.S. developed the sampling probes, performed surgeries and experiments, and wrote the manuscript under the direction of R.T.K. O.S.M. helped to design and implement the LC-MS methods and revised the manuscript. K.A.P.-S. performed histology and assisted with statistics under the direction of B.J.A.

Funding

National Institute of Health 5R37EB003320 and The McKnight Foundation provided funding for this work.

Notes

The authors declare no competing financial interest.

■ ACKNOWLEDGMENTS

We wish to thank Alexandra Difeliceantonio for assistance with histology. We also wish to thank Francis Esmonde-White for his help with MATLAB and many helpful discussions.

■ ABBREVIATIONS

3-MT, 3-methoxytyramine; 5-HIAA, 5-hydroxyindoleacetic acid; 5-HT, serotonin; ACh, acetylcholine; Asp, aspartic acid; COMT, catechol-*O*-methyltransferase; DA, dopamine; DAT, dopamine transporter; DOPAC, 3,4-dihydroxyphenylacetic acid; GABA, γ-aminobutyric acid; Glu, glutamic acid; Gly, glycine; HVA, homovanillic acid; ID, inner diameter; MAO, monoamine oxidase; NE, norepinephrine; NM, normetanephrine; NNF, "no-net-flux"; OD, outer diameter; SEM, standard error of the mean; VTA, ventral tegmental area

■ REFERENCES

(1) Peciña, S., and Berridge, K. C. (2005) Hedonic Hot Spot in Nucleus Accumbens Shell: Where Do μ-Opioids Cause Increased Hedonic Impact of Sweetness? *J. Neurosci. 25*, 11777−11786.

(2) Brown, P., and Molliver, M. E. (2000) Dual Serotonin (5-HT) Projections to the Nucleus Accumbens Core and Shell: Relation of the 5-HT Transporter to Amphetamine-Induced Neurotoxicity. *J. Neurosci. 20*, 1952−1963.

(3) Van Bockstaele, E. J., and Pickel, V. M. (1993) Ultrastructure of serotonin-immunoreactive terminals in the core and shell of the rat nucleus accumbens: Cellular substrates for interactions with catecholamine afferents. *J. Comp. Neurol. 334*, 603−617.

(4) Willoughby, J., Glover, V., and Sandler, M. (1988) Histochemical localisation of monoamine oxidase A and B in rat brain. *J. Neural Transm. 74*, 29−42.

(5) Baldo, B. A., Daniel, R. A., Berridge, C. W., and Kelley, A. E. (2003) Overlapping distributions of orexin/hypocretin- and dopamine-β-hydroxylase immunoreactive fibers in rat brain regions mediating arousal, motivation, and stress. *J. Comp. Neurol. 464*, 220−237.

(6) Bubar, M. J., Stutz, S. J., and Cunningham, K. A. (2011) 5-HT_{2C} Receptors Localize to Dopamine and GABA Neurons in the Rat Mesoaccumbens Pathway. *PLoS One 6*, e20508.

(7) Yung, K. K. L., Bolam, J. P., Smith, A. D., Hersch, S. M., Ciliax, B. J., and Levey, A. I. (1995) Immunocytochemical localization of D1 and D2 dopamine receptors in the basal ganglia of the rat: Light and electron microscopy. *Neuroscience 65*, 709−730.

(8) Freed, C., Revay, R., Vaughan, R. A., Kriek, E., Grant, S., Uhl, G. R., and Kuhar, M. J. (1995) Dopamine transporter immunoreactivity in rat brain. *J. Comp. Neurol. 359*, 340−349.

(9) Miner, L. H., Schroeter, S., Blakely, R. D., and Sesack, S. R. (2003) Ultrastructural localization of the norepinephrine transporter in superficial and deep layers of the rat prelimbic prefrontal cortex and its spatial relationship to probable dopamine terminals. *J. Comp. Neurol. 466*, 478−494.

(10) Kalivas, P. W. (2009) The glutamate homeostasis hypothesis of addiction. *Nat. Rev. Neurosci. 10*, 561−572.

(11) Knackstedt, L. A., LaRowe, S., Mardikian, P., Malcolm, R., Upadhyaya, H., Hedden, S., Markou, A., and Kalivas, P. W. (2009) The Role of Cystine-Glutamate Exchange in Nicotine Dependence in Rats and Humans. *Biol. Psychiatry 65*, 841−845.

(12) Westerink, B. H. C., and Timmerman, W. (1999) Do neurotransmitters sampled by brain microdialysis reflect functional release? *Anal. Chim. Acta 379*, 263−274.

(13) Fuxe, K., Dahlstroem, A. B., Jonsson, G., Marcellino, D., Guescini, M., Dam, M., Manger, P., and Agnati, L. (2010) The discovery of central monoamine neurons gave volume transmission to the wired brain. *Prog. Neurobiol. (Amsterdam, Neth.) 90*, 82−100.

(14) Nandi, P., and Lunte, S. M. (2009) Recent trends in microdialysis sampling integrated with conventional and microanalytical systems for monitoring biological events: A review. *Anal. Chim. Acta 651*, 1−14.

(15) Robinson, D. L., Hermans, A., Seipel, A. T., and Wightman, R. M. (2008) Monitoring Rapid Chemical Communication in the Brain. *Chem. Rev. 108*, 2554−2584.

(16) Park, J., Aragona, B. J., Kile, B. M., Carelli, R. M., and Wightman, R. M. (2010) In vivo voltammetric monitoring of catecholamine release in subterritories of the nucleus accumbens shell. *Neuroscience 169*, 132−142.

(17) Robinson, D. L., Howard, E. C., McConnell, S., Gonzales, R. A., and Wightman, R. M. (2009) Disparity Between Tonic and Phasic Ethanol-Induced Dopamine Increases in the Nucleus Accumbens of Rats. *Alcohol.: Clin. Exp. Res. 33*, 1187−1196.

(18) Robinson, D. L., Venton, B. J., Heien, M. L. A. V., and Wightman, R. M. (2003) Detecting Subsecond Dopamine Release with Fast-Scan Cyclic Voltammetry in Vivo. *Clin. Chem. 49*, 1763−1773.

(19) Kottegoda, S., Shaik, I., and Shippy, S. A. (2002) Demonstration of low flow push-pull perfusion. *J. Neurosci. Methods 121*, 93−101.

(20) Gaddum, J. H. (1961) Push-Pull Cannulae. *J. Physiol. (London, U.K.) 155*, 1P−2P.

(21) Slaney, T. R., Nie, J., Hershey, N. D., Thwar, P. K., Linderman, J., Burns, M. A., and Kennedy, R. T. (2011) Push-Pull Perfusion Sampling with Segmented Flow for High Temporal and Spatial Resolution in Vivo Chemical Monitoring. *Anal. Chem. 83*, 5207−5213.

(22) Cellar, N. A., Burns, S. T., Meiners, J. C., Chen, H., and Kennedy, R. T. (2005) Microfluidic Chip for Low-Flow Push-Pull Perfusion Sampling in Vivo with On-Line Analysis of Amino Acids. *Anal. Chem. 77*, 7067−7073.

(23) Cellar, N. A., and Kennedy, R. T. (2006) A capillary-PDMS hybrid chip for separations-based sensing of neurotransmitters in vivo. *Lab Chip 6*, 1205−1212.

(24) Song, P., Mabrouk, O. S., Hershey, N. D., and Kennedy, R. T. (2012) In Vivo Neurochemical Monitoring Using Benzoyl Chloride Derivatization and Liquid Chromatography-Mass Spectrometry. *Anal. Chem. 84*, 412−419.

(25) Lin, Z., Canales, J. J., Bjorgvinsson, T., Thomsen, M., Qu, H., Liu, Q.-R., Torres, G. E., Caine, S. B., and Shafiqur, R. (2011) Monoamine Transporters: Vulnerable and Vital Doorkeepers. In *Progress in Molecular Biology and Translational Science*, Chapter 1, Vol. 98, pp 1−46, Academic Press: London, UK.

(26) Ikemoto, S. (2010) Brain reward circuitry beyond the mesolimbic dopamine system: A neurobiological theory. *Neurosci. Biobehav. Rev. 35*, 129−150.

(27) McKittrick, C. R., and Abercrombie, E. D. (2007) Catecholamine mapping within nucleus accumbens: differences in basal and amphetamine-stimulated efflux of norepinephrine and dopamine in shell and core. *J. Neurochem. 100*, 1247−1256.

(28) Owesson-White, C. A., Roitman, M. F., Sombers, L. A., Belle, A. M., Keithley, R. B., Peele, J. L., Carelli, R. M., and Wightman, R. M. (2012) Sources contributing to the average extracellular concentration of dopamine in the nucleus accumbens. *J. Neurochem. 121*, 252−262.

(29) Heidbreder, C., and Feldon, J. (1998) Amphetamine-induced neurochemical and locomotor responses are expressed differentially across the anteroposterior axis of the core and shell subterritories of the nucleus accumbens. *Synapse 29*, 310−322.

(30) Aragona, B. J., Cleaveland, N. A., Stuber, G. D., Day, J. J., Carelli, R. M., and Wightman, R. M. (2008) Preferential enhancement of dopamine transmission within the nucleus accumbens shell by cocaine is attributable to a direct increase in phasic dopamine release events. *J. Neurosci. 28*, 8821−8831.

(31) Aragona, B. J., Day, J. J., Roitman, M. F., Cleaveland, N. A., Wightman, R. M., and Carelli, R. M. (2009) Regional specificity in the real-time development of phasic dopamine transmission patterns during acquisition of a cue-cocaine association in rats. *Eur. J. Neurosci. 30*, 1889−1899.

(32) Lammel, S., Hetzel, A., Häckel, O., Jones, I., Liss, B., and Roeper, J. (2008) Unique Properties of Mesoprefrontal Neurons

within a Dual Mesocorticolimbic Dopamine System. *Neuron 57*, 760−773.
(33) Richardson, R. R., Jr., Miller, J. A., and Reichert, W. M. (1993) Polyimides as biomaterials: preliminary biocompatibility testing. *Biomaterials 14*, 627−635.
(34) Szerb, J. C. (1967) Model Experiments with Gaddum's Push-Pull Cannulas. *Can. J. Physiol. Pharmacol. 45*, 613−620.
(35) Nicholson, C., and Phillips, J. M. (1981) Ion diffusion modified by tortuosity and volume fraction in the extracellular microenvironment of the rat cerebellum. *J. Physiol. (London, U.K.) 321*, 225−257.
(36) Höistad, M., Chen, K. C., Nicholson, C., Fuxe, K., and Kehr, J. (2002) Quantitative dual-probe microdialysis: evaluation of [^{3}H]-mannitol diffusion in agar and rat striatum. *J. Neurochem. 81*, 80−93.
(37) Rice, M. E., Patel, J. C., and Cragg, S. J. (2011) Dopamine release in the basal ganglia. *Neuroscience 198*, 112−137.
(38) Tang, A., Bungay, P. M., and Gonzales, R. A. (2003) Characterization of probe and tissue factors that influence interpretation of quantitative microdialysis experiments for dopamine. *J. Neurosci. Methods 126*, 1−11.
(39) Abercrombie, E. D., Keefe, K. A., Difrischia, D. S., and Zigmond, M. J. (1989) Differential Effect of Stress on in Vivo Dopamine Release in Striatum, Nucleus Accumbens, and Medial Frontal-Cortex. *J. Neurochem. 52*, 1655−1658.
(40) Wood, P. L., and Altar, C. A. (1988) Dopamine release in vivo from nigrostriatal, mesolimbic, and mesocortical neurons: utility of 3-methoxytyramine measurements. *Pharmacol. Rev. 40*, 163−187.
(41) Roffler-Tarlov, S., Sharman, D. F., and Tegerdine, P. (1971) 3,4-Dihydroxyphenylacetic acid and 4-hydroxy-3-methoxyphenylacetic acid in the mouse striatum: a reflection of intra- and extra-neuronal metabolism of dopamine? *Br. J. Pharmacol. 42*, 343−351.
(42) Bast, T., Diekamp, B., Thiel, C., Schwarting, R. K. W., and Gunturkun, O. (2002) Functional aspects of dopamine metabolism in the putative prefrontal cortex analogue and striatum of pigeons (Columba livia). *J. Comp. Neurol. 446*, 58−67.
(43) Hardebo, J. E., and Owman, C. H. (1980) Characterization of the in vitro uptake of monoamines into brain microvessels. *Acta Physiol. Scand. 108*, 223−229.
(44) Tanahashi, S., Ueda, Y., Nakajima, A., Yamamura, S., Nagase, H., and Okada, M. (2012) Novel δ1-receptor agonist KNT-127 increases the release of dopamine and l-glutamate in the striatum, nucleus accumbens and median pre-frontal cortex. *Neuropharmacology 62*, 2057−2067.
(45) Moroni, F., Cozzi, A., Carpendo, R., Cipriani, G., Veneroni, O., and Izzo, E. (2005) Kynurenine 3-mono-oxygenase inhibitors reduce glutamate concentration in the extracellular spaces of the basal ganglia but not in those of the cortex or hippocampus. *Neuropharmacology 48*, 788−795.
(46) Lehre, K. P., Levy, L. M., Ottersen, O. P., Storm-Mathisen, J., and Danbolt, N. C. (1995) Differential expression of two glial glutamate transporters in the rat brain: quantitative and immunocytochemical observations. *J. Neurosci. 15*, 1835−1853.
(47) D'Este, L., Casini, A., Puglisi-Allegra, S., Cabib, S., and Renda, T. G. (2007) Comparative immunohistochemical study of the dopaminergic systems in two inbred mouse strains (C57BL/6J and DBA/2J). *J. Chem. Neuroanat. 33*, 67−74.
(48) Sato, H., Tamba, M., Okuno, S., Sato, K., Keino-Masu, K., Masu, M., and Bannai, S. (2002) Distribution of Cystine/Glutamate Exchange Transporter, System x_c^-, in the Mouse Brain. *J. Neurosci. 22*, 8028−8033.
(49) Herrera-Marschitz, M., You, Z. B., Goiny, M., Meana, J. J., Silveira, R., Godukhin, O. V., Chen, Y., Espinoza, S., Pettersson, E., Loidl, C. F., Lubec, G., Andersson, K., Nylander, I., Terenius, L., and Ungerstedt, U. (1996) On the Origin of Extracellular Glutamate Levels Monitored in the Basal Ganglia of the Rat by In Vivo Microdialysis. *J. Neurochem. 66*, 1726−1735.
(50) David, D. J., Zahniser, N. R., Hoffer, B. J., and Gerhardt, G. A. (1998) *In Vivo* Electrochemical Studies of Dopamine Clearance in Subregions of Rat Nucleus Accumbens: Differential Properties of the Core and Shell. *Exp. Neurol. 153*, 277−286.
(51) Wightman, R. M., Heien, M. L. A. V., Wassum, K. M., Sombers, L. A., Aragona, B. J., Khan, A. S., Ariansen, J. L., Cheer, J. F., Phillips, P. E. M., and Carelli, R. M. (2007) Dopamine release is heterogeneous within microenvironments of the rat nucleus accumbens. *Eur. J. Neurosci. 26*, 2046−2054.
(52) Valentini, V., Frau, R., Bordi, F., Borsini, F., and Di Chiara, G. (2011) A microdialysis study of ST1936, a novel 5-HT6 receptor agonist. *Neuropharmacology 60*, 602−608.
(53) Watson, C. J., Venton, B. J., and Kennedy, R. T. (2006) In Vivo Measurements of Neurotransmitters by Microdialysis Sampling. *Anal. Chem. 78*, 1391−1399.
(54) Justice, J. B., Jr (1993) Quantitative microdialysis of neurotransmitters. *J. Neurosci. Methods 48*, 263−276.
(55) Engleman, E. A., Keen, E. J., Tilford, S. S., Thielen, R. J., and Morzorati, S. L. (2011) Ethanol drinking reduces extracellular dopamine levels in the posterior ventral tegmental area of non-dependent alcohol-preferring rats. *Alcohol 45*, 549−557.
(56) Crippens, D., Camp, D. M., and Robinson, T. E. (1993) Basal extracellular dopamine in the nucleus accumbens during amphetamine withdrawal: a "no net flux" microdialysis study. *Neurosci. Lett. 164*, 145−148.
(57) Smith, A. D., and Weiss, F. (1999) Ethanol Exposure Differentially Alters Central Monoamine Neurotransmission in Alcohol-Preferring versus -Nonpreferring Rats. *J. Pharmacol. Exp. Ther. 288*, 1223−1228.
(58) Katner, S. N., and Weiss, F. (2001) Neurochemical Characteristics Associated With Ethanol Preference in Selected Alcohol-Preferring and -Nonpreferring Rats: A Quantitative Microdialysis Study. *Alcohol.: Clin. Exp. Res. 25*, 198−205.
(59) Chen, N. N. H., Lai, Y.-J., and Pan, W. H. T. (1997) Effects of different perfusion medium on the extracellular basal concentration of dopamine in striatum and medial prefrontal cortex: a zero-net flux microdialysis study. *Neurosci. Lett. 225*, 197−200.
(60) Sam, P. M., and Justice, J. B. (1996) Effect of General Microdialysis-Induced Depletion on Extracellular Dopamine. *Anal. Chem. 68*, 724−728.
(61) Tao, R., Ma, Z., and Auerbach, S. B. (2000) Differential Effect of Local Infusion of Serotonin Reuptake Inhibitors in the Raphe versus Forebrain and the Role of Depolarization-Induced Release in Increased Extracellular Serotonin. *J. Pharmacol. Exp. Ther. 294*, 571−579.
(62) Redgrave, P. (1977) A modified push-pull system for the localised perfusion of brain tissue. *Pharmacol., Biochem. Behav. 6*, 471−474.
(63) Paxinos, G., and Watson, C. (2008) *The Rat Brain in Stereotaxic Coordinates*, Academic Press, San Diego, CA.